Ecological Indicators 141 (2022) 109075

Contents lists available at ScienceDirect

Ecological Indicators

journal homepage: www.elsevier.com/locate/ecolind

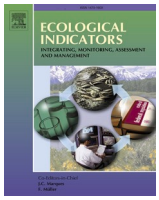

The microalgae *Chaetoceros tenuissimus* exposed to contaminants of emerging concern: A potential alternative to standardized species for marine quality assessment

Paolo Pastorino [a,*,1], Andrea Broccoli [b,1], Serena Anselmi [b], Elisa Bagolin [c], Marino Prearo [a], Damià Barceló [d,e], Monia Renzi [c]

[a] Istituto Zooprofilattico Sperimentale del Piemonte, Liguria e Valle d'Aosta, 10154 Torino, Italy
[b] Bioscience Research Center, 58015 Orbetello, Italy
[c] Dipartimento di Scienze della Vita, Università degli Studi di Trieste, 34127 Trieste, Italy
[d] Catalan Institute for Water Research (ICRA-CERCA), 17003 Girona, Spain
[e] Institute of Environmental Assessment and Water Research (IDAEA-CSIC), 08034 Barcelona, Spain

ARTICLE INFO

Keywords:
Chaetoceros tenuissimus
Chlorophyll
Growth response
Nanoparticles
Surfactant
Water quality assessment

ABSTRACT

Microalgae occupy a key trophic level since primary producers at the base of the aquatic food chain. Moreover, they are well suited for ecotoxicological tests because easily cultured and sensitive to contaminants. However, species sensitiveness to the same chemicals can vary greatly. Thus, we characterized the non-standardized diatom *Chaetoceros tenuissimus* by means of growth inhibition, biochemical, and infrared-spectroscopy (FT-IR) tests and compared the results against the standardized diatom *Phaeodactylum tricornutum*. The two species were exposed for 72 h to four chemicals: nanoparticles (n-TiO_2, n-ZnO), potassium dichromate ($K_2Cr_2O_7$), and surfactant (polyethylene glycol; PEG). The sensitivity of *C. tenuissimus* in the growth inhibition test and the chlorophyll-*a* analysis was always higher than *P. tricornutum*. In particular, the chlorophyll-*a* analysis exhibited an earlier endpoint for *C. tenuissimus* exposed to all chemicals here considered. FT-IR showed spectral alterations (molecular changes in chlorophyll) in both microalgal species exposed to the chemicals compared to the negative controls, with stronger alterations in *C. tenuissimus* than *P. tricornutum*. In conclusion, *C. tenuissimus* showed higher sensitivity to a broad range of toxic chemicals, indicating the potential use of this species in marine quality assessment as an alternative to the standardized *P. tricornutum*.

1. Introduction

Microalgae inhabit the world's oceans and seas where they occupy a key trophic level in aquatic ecosystems as primary producers at the base of the marine food chain (Mucha et al., 2003). Their turnover rate is 10 times faster than that of multicellular aquatic producers (Shurin et al., 2006). Because physical and chemical impacts on aquatic ecosystems can have bottom-up effects for organisms higher in the trophic web (Li et al., 2020), phytoplankton have long been used as an effective bioindicator of environmental quality (Parmar et al., 2016; Rao et al., 2018), for instance, water, effluent waste quality, and environmental risk (Gomaa et al., 2021; Wang et al., 2021).

Generally, organisms for a bioassay should be widespread in an ecosystem, ecologically relevant, sensitive to contaminants, and easy to handle and maintain in the laboratory (EPA, 1991; Mecozzi et al., 2008; Luan et al., 2020). Owing to their sensitivity to pollutants, ecological relevance, and ease of culturing and maintaining under laboratory conditions, microalgae provide a model organism in ecotoxicology according to international standardization under UNI EN ISO 10253:2017 (ISO, 2017).

Commonly used algal species (diatoms: *Phaeodactylum tricornutum, Skeletonema* sp.; Chlorophyceae: *Pseudokirchneriella subcapitata*, *Dunaliella tertiolecta, Scenedesmus quadricauda*; Prymnesiophyceae: *Isochrysis* sp.) in bioassays meet these requisites (ISO, 2017).

Moreover, microalgae can serve as a proxy of marine water quality by virtue of their ability to respond rapidly (72 h) to a varied range of

* Corresponding author.
E-mail address: paolo.pastorino@izsto.it (P. Pastorino).
[1] These authors contributed equally.

https://doi.org/10.1016/j.ecolind.2022.109075
Received 10 May 2022; Received in revised form 10 June 2022; Accepted 14 June 2022
Available online 18 June 2022

contaminants, providing early warning signals of environmental change and cues for identifying its potential causes (McCormick and Cairns, 1994; Singh and Patidar, 2018; Rodrigues et al., 2021). For example, fresh and brackish algal mixture cultures can be used for predicting environmental quality (Pastorino et al., 2021), while monospecific algal cultures find broad use as bioindicators in ecotoxicology, where their response can be observed at various levels of biological organization (Puiseux-Dao, 2018). Ecotoxicological tests (and bioassays) on many algal species are standardized by the National and International Organization for Standardization (ISO, 2017) and the Organization for Economic Cooperation and Development (OECD, 2000). Such tests may use phytoplankton inhibition of growth rate as an endpoint (response) to chemical stress (Häder and Gao, 2015) for standardized measurement of aquatic status.

In the search for supplementary sensitive methods to assess early response (by morphological or physiological observation) in microalgae species, Renzi et al. (2014) and Broccoli et al. (2021) reported that the sublethal effects observed in marine algal species *Phaeodactylum tricornutum, Isochryris galbana,* and freshwater species *Pseudokirchneriella subcapitata* and *Scenedesmus quadricauda*, based on the quantification of chlorophyll-*a* by conventional spectroscopy and biovolume by field emission-scanning electron microscopy, allows for a more powerful recognition of potential effects on aquatic ecosystems than the standardized inhibition of growth endpoints (Renzi et al., 2014).

Another little studied endpoint is micro-Fourier transform infrared spectrum (μFT-IR) spectroscopy, in which algal culture (or their extracts) is a good proxy of biomolecular composition (carbohydrates, proteins, lipids, nucleic acids). The IR spectrum of cultures exposed to toxicants can differ from negative control culture, as observed in the tissues of many organisms (Beleites et al., 2005; Yu and Irudayaraj, 2005).

The fitness of phytoplankton communities decreases after exposure to chemicals and contaminants of emerging concern (CECs) that impact on aquatic ecosystems (Pastorino et al., 2021). Contaminants of emerging concern emitted by municipal wastewater systems have an ecological impact on aquatic environments (Pastorino and Ginebreda, 2021); however, published studies of the effects that these chemicals have on phytoplankton species are still scant to date.

Nanoparticles (1–100 nm) includes a heterogeneous group of chemicals (Besha et al., 2020). Zinc oxide (ZnO) and titanium dioxide (TiO_2) nanoparticles are pervasive in the environment (Renzi and Guerranti, 2015; Prajitha et al., 2019). They can be found in industrial products (Turan et al., 2019), medicines, personal care products, rubber, glass, plastic, and paints (Turan et al., 2019).

Chromium (Cr), a natural metal found in the environment in trivalent Cr (III) and hexavalent Cr (VI) valence states, is commonly used in laboratory procedures as positive control of tests (e.g., ISO, 2016) and in numerous industrial processes. Indeed, commercial chromium compounds are used in industrial welding, metal finishes, leather tanning, and wood preservation. Studies of this non-negligible pollutant in microalgae found harmful effects of Cr (VI) (Labra et al., 2007; Yamagishi et al., 2017). Potassium dichromate ($K_2Cr_2O_7$) is now considered a CEC since it was recently detected in watercourses at concentrations significantly higher than expected (Benjamin and Kutty, 2019). Indeed, it is widely employed as a reagent in industrial (colouring, printing, electroplating, pyrotechnics) and laboratory applications (analytical reagent) in various countries (Benjamin and Kutty, 2019).

Surfactants are amphiphilic molecules with a hydrophobic and a hydrophilic part that in aqueous solution frequently assemble at interfaces and self-associate to sequester their apolar regions from contact with the aqueous phase (Lawrence, 1994). Polyethylene glycol (PEG) is employed as a surfactant in the pharmaceutical industry, in veterinary drugs, in industrial and other applications such as detergents, printing and chemical mixtures (Jang et al., 2015). Little is known about the toxicological properties of PEG (Nascimento et al., 2021).

Different species, at the same conditions or in the same environment, can differ in their sensitivity to a specific toxic substance. Interspecies sensitivity to environmental contaminants (e.g., toxicity level) depends on cellular receptors (or targets) of contaminants, differences in uptake rate, and detoxification mechanisms (Levy et al., 2007); while some species may show effects in survivors, others may have no observable effects (Fleeger et al., 2003; Krull and Barros, 2012) or show hormesis (Agathokleous et al., 2021).

Depending on the species observed and its relative sensitivity to a specific contaminant, microalgal bioindicators can produce false results about the bioavailability of a contaminant; as such they may not measure the real effect of toxicity in the environment (McPherson and Chapman, 2000; Krull and Barros, 2012) and the quality of an aquatic ecosystem. By performing tests on unstandardized algal species, we may discover ones that are more sensitive (and simpler to culture and handle) and that better discriminate potentially toxic events early. With this hypothesis in mind, we performed growth inhibition tests, biochemical and infrared spectroscopy analysis on the diatom *Chaetoceros tenuissimus* and compared the results with the standardized diatom *Phaeodactylum tricornutum* to characterize it for its potential application in marine environmental quality assessment.

Chaetoceros tenuissimus (Bacillariophyta, Centrales) was selected since it can be easily found in the Mediterranean Sea, Atlantic Ocean, Japanese coastal waters, and other many places (Hongo et al., 2021). This species has a high growth rate (at least three divisions per day) and blooms occur throughout the spring and autumn (Hongo et al., 2021). Generally, literature on *C. tenuissimus* is scant for genotoxicity (Desai et al., 2006, Deasi et al., 2010; Sarker et al., 2016), metabolomics analysis (Hano and Tomaru, 2019), and pathogenicity (Tomaru et al., 2011), and analysis of growth inhibition tests, biochemical, and molecular changes is completely lacking. To fill this knowledge gap, we performed tests using four CECs: nanoparticles (n-ZnO, n-TiO_2), potassium dichromate ($K_2Cr_2O_7$), and surfactant (polyethylene glycol).

2. Material and methods

2.1. Experimental design

Two marine algal species, the unstandardized (and less studied) species *Chaetoceros tenuissimus* and the standardized species *Phaeodactylum tricornutum*, were exposed to four CECs. Effects of exposure were measured according to ecotoxicological tests (ISO, 2017). The two species in the exponential growth phase were exposed to various concentrations of nanoparticles (n-ZnO, n-TiO_2), $K_2Cr_2O_7$, and surfactant (polyethylene glycol) to determine the half maximal effective concentration (EC_{50}) after 72 h of exposure (under controlled environmental conditions) compared to negative controls (algal cultures not exposed to the chemicals). The endpoints were growth inhibition and photosynthetic complex efficiency (biochemical analysis; spectrophotometry). Molecular changes were also evaluated in the chlorophyll extract in acetone (μFT-IR microscopy).

2.2. Collection of algal species

The algal species *Chaetoceros tenuissimus* was isolated by serial dilution from natural brackish water the Orbetello Lagoon and treated with antibiotics (amoxicillin 25 mg/L) to produce an axenic culture following the protocol proposed by Spilling (2020). *Phaeodactylum tricornutum* was collected from *in vitro* conditions by a stock batch (Ecotox Ltd, Tavistock, UK).

2.3. Chemicals and concentrations

Four CECs of high ecological impact were used for the purpose of this study: n-ZnO (CAS n. 1314–13-2, powder, particle size < 100 nm, surface area 15–25 m^2/g, Caelo Hilden, Germany); n-TiO_2 (CAS n. 13463–67-7, powder, particle size < 21 nm, surface area 35–65 m^2/g,

Caelo, Hilden, Germany); $K_2Cr_2O_7$ (pharmaceutical powder, EG S.p.A., Milan, Italy), and polyethylene glycol (PEG 400; CAS n. 25322–68-3, pure liquid, Farmalabor, Canosa di Puglia, Italy). Exposure concentrations were determined considering both pilot tests to define the correct range dilutions and main literature (Wang et al., 2016; Benjamin and Kutty, 2019; Joonas et al., 2019; Nascimento et al., 2021). EC_{50} was calculated using the following chemical concentrations: 10, 25, 50, 100, 200, 300.0 mg/L (n-TiO_2); 10, 25, 50, 100, 200, 300 mg/L (n-ZnO); 3.2, 5.6, 10, 18, 32, 50 mg/L ($K_2Cr_2O_7$); 10, 25, 50, 100, 250, 500 mg/L (polyethylene glycol).

Nanoparticles were the same as those tested by Renzi and Blašković (2019) and Broccoli et al. (2021). The stock suspension of 500 mg/L n-ZnO and 500 mg/L n-TiO_2 were prepared with Millipore water and treated by sonication with a power of 40 Hz for 20 min to disaggregate micrometric clusters that were present in untreated dust. The suspension was placed in an ultrasound water bath for 30 min before being diluted to different exposure concentrations (Tang et al., 2018). After sonication treatment, an aliquot of the suspension (both for n-ZnO and n-TiO_2), at concentration of 300 mg/L, 100 mg/L, and 10 mg/L (exposure concentrations), respectively, was put in a disposable polystyrene cuvette to determine particle size with FESEM microscopy (Zeiss, 158 mod. Merlin II + WD/ED combined microanalyzer).

To mimic the dissolution of nanoparticles (NPs) in toxicity testing environment, the protocol proposed by Wu et al. (2019) was strictly followed. Briefly, n-TiO_2 and n-ZnO suspensions (300 mg/L, 100 mg/L, and 10 mg/L; in triplicates) in algal medium (ASTM medium) were prepared and incubated in the same conditions as for algal toxicity testing (see section 2.4.). Zinc, titanium, and chromium concentrations were determined after 72 h in each suspension by inductively coupled plasma-mass spectrometry (ICP-MS Xseries II, Thermo Scientific, Bremen, Germany). Analytical performance was verified by processing certified reference materials (SRM 1566b), along with blank reagents in each analytical session. The limit of quantification (LOQ) was 0.005 mg/L for Ti, 0.015 mg/L for Zn and 0.012 mg/L for Cr.

Analytical determination of PEG was also performed in each suspension based on the Dragendorff reagent method (Nascimento et al., 2021). Briefly, Dragendorff reagent was prepared with 5 mL of bismuth oxide, 5 mL of potassium iodide and 90 mL of purified water. Then, 10 mL of samples were mixed to 40 mL of PBS, 40 mL of HCl and 100 mL of the Dragendorff reagent. Subsequently, the solution was pipetted into an ELISA microplate (read at 492 nm, in ELISA reader) after the reagent was homogenized in a vortex. Simultaneously, a standard curve was plotted based on different PEG concentrations diluted in PBS. The equation of the obtained line was used to determine PEG concentrations in the samples.

2.4. Growth inhibition tests

In both algal species, standardized ecotoxicological tests (ISO, 2017) were performed with few modifications (using ASTM algal medium); controlled and standardized variables were settled and constantly monitored (medium salinity 30 ± 1 ‰; temperature 20 ± 2 °C; pH 8.0 ± 0.2; illumination 12 light and 12 dark; 10 k lux from both sides).

The endpoint of this analysis was inhibition of growth of the algal species after exposure to a chemical. Both species (10 replicates) in their exponential growth phase were exposed to the chemical for 72 h. Cell density was measured by spectrophotometry (Inno spectrophotometer, optical length 1 cm, LTek Co. Ltd, Republic of Korea) of light absorbance at 670 nm wavelength, every 24 h for 72 h. Spectrophotometric measurement was correlated to cell density to determine a calibration curve performed with Thoma's chamber for the analyses. The samples (chemicals and negative controls) were added with nutrients and enough algal culture to reach 10^4 cells/mL. After 72 h of exposure the growth rate (μ) and the growth inhibition percentage (I%) were calculated by formulae previously reported (Aravantinou et al., 2015). The growth inhibition percentage was the main endpoint of the test; it indicated the logarithmic increase in biomass (based on growth rate) during 72 h of exposure (OECD, 2011). Based on the average inhibition growth percentage in the dilutions, the concentration (mg/L) was calculated that determines 50% of growth inhibition (EC_{50}) and was compared to the negative controls (ASTM cell culture medium; 10 replicates).

Tests were performed following the general quality criteria applied by the laboratory including positive (n = 10) and negative (n = 10) controls during experiments and a metrologically traceable approach based on the use of LAT calibrated instrumentation. According to UNI EN ISO 10253:2017 (ISO, 2017), standardized reference values are available for *Phaeodactylum tricornutum*. The tests were considered valid if the algal growth rate of the negative control after 72 h of growth was > 16 times the starting algal concentration. Moreover, the tests are considered valid if the EC_{50} of the positive controls, performed with potassium dichromate, was 20.1 ± 5.3 mg/L (ISO, 2017).

2.5. Determination of chlorophylls levels

Chlorophylls (Chl *a, c*) were analysed according to the APAT CNR IRSA 9020 method (APAT, 2003) at the end of the inhibition of algal growth (after 72 h). Chl-*b* was not determined since not present in the diatom species (Kuczynska et al., 2015). A volume of 6 mL of algal species of each sample (n = 10) was filtered on glass fibre filters (0.45 μm ø pore) by vacuum pump. The cultures on the filter were then extracted with analytic grade acetone (Sigma Aldrich, St. Louis, MO. USA) and kept on ice and in the dark for 2 h to avoid chemical degradation. The supernatant was collected, and spectrophotometric absorbance (Onda UV-30 UV/Vis spectrophotometer, optical length 1 cm, Bormac, Carpi, Italy) was measured at 630, 647, 664, and 750 nm. Chlorophyll-*a* and Chl-*c* concentrations (mg/m3) were calculated following the formulae reported by Broccoli et al. (2021). The limit of quantification (LOQ) was 0.001 mg/m^3. The percentage of Chl-*a*, *c* was used to determine the EC_{50} for the chlorophylls (photosynthetic complex efficiency).

2.6. Molecular changes

In order to determine molecular changes in the chlorophyll (extracts) and calculate the percentage of spectral match between the exposed and the negative control cultures the Fourier transformed infrared spectroscopy (μFT-IR) was used. A drop of extract was placed on a gold slide, air-dried (35 °C), and quantified by μFT-IR microscopy (Nicolet iN10 MX μFT-IR microscope, Thermo Fisher Scientific, Waltham, MA, USA) equipped with a liquid nitrogen-cooled MCT-A. The spectral readings were collected from 10 replicates by reflection mode (range 4000–670 cm^{-1}) to determine the mean spectra of the cultures using Omnic™ Picta™ software (Thermo Fisher Scientific). Mean matches (%) were calculated using Omnica™ Specta™ by averaging the matches of the spectral replicates (single spectra collected per type, n = 10). To obtain a mean spectrum for each condition and for comparison to the negative controls, the peak height in absorbance at each wavelength was calculated (Mecozzi et al., 2008). Single peaks (regions) of the spectra between the exposed culture and the negative controls were compared to determine the influence of each on the whole spectrum matches calculated previously. Regions of spectra were selected based on the peaks and the relevant differences in observed trend shape. Range of spectra: 1 = 675 – 771 cm^{-1}, 2 = 775 – 933 cm^{-1}, 3 = 937 – 1188 cm^{-1}, 4 = 1192 – 1331 cm^{-1}, 5 = 1342 – 1481 cm^{-1}, 6 = 1504 – 1813 cm^{-1}, 7 = 2307 – 2411 cm^{-1}, 8 = 2831 – 3066 cm^{-1}, 9 = 3225 – 3741 cm^{-1}.

2.7. Quality assurance and quality control (QA/QC)

During the experiments, a strict QA/QC process was used to assure the methodological quality of the results. Bioscience Research Centre is an ISO 9001:2015 certified laboratory that follows control procedures

reported by UNI EN ISO 17025:2018 (ISO, 2018).

2.8. Statistical analyses

Data normality and homoscedasticity were assessed through the Shapiro-Wilk and Levene tests, respectively. Descriptive statistical analysis was performed using Excel® software (Microsoft, Redmond, WA, USA). Results are expressed as mean, standard deviation (SD) and percentage. Algal growth inhibition (EC_{50}) was calculated for each chemical by running Toxicity Response Analysis Program-TRAP® software (regression analysis plots), while the biomarker EC_{50} was calculated using the AAT tool (ATT Bioquest, Sunnyvale, CA, USA) (2021, May 20) Quest Graph™ EC_{50} calculator.

Principal component analysis (PCA) was performed to check for trends in molecular changes (μFT-IR analyses) of both controls (unexposed cultures) and cultures exposed to chemicals (n-TiO_2, n-ZnO, $K_2Cr_2O_7$, PEG). The results of PCA were plotted by summarizing the molecular effects of the chemicals; the idea was to simplify and verify the alterations in the two algal species and the four chemicals. Since the null hypothesis for the homogeneity of variance and/or for normal distribution could not be rejected, the Kruskal–Wallis test was performed to disclose statistically significant differences in biochemical biomarkers (chlorophylls) between the exposed and the control microalgae cultures. Dunn's was used as a post-hoc test to compare the exposed microalgae cultures with the negative controls. Statistical analysis was performed using XLSTAT (XLSTAT - NY, USA, 2020).

2.9. Nanoparticle characterization and dissolution of chemicals in algal medium

ZnO NPs measured showed cubic and parallelepiped shapes with a mean dimension (mean ± standard deviation; n = 30) of 58.5 ± 18.4 nm × 77.7 ± 27.0 nm (cubic) and 208.1 ± 143.3 nm × 328.8 ± 132.2 nm (parallelepiped). The mean length and width (mean ± standard deviation; n = 30) of TiO_2 NPs were 54 ± 18 nm and 36.25 ± 11.62 nm, respectively. The concentrations of the released Ti were lower than the LOQ (0.005 mg/L) in both 25 and 10 mg/L suspensions. The highest TiO_2 NPs solutions (100, 200, and 300 mg/L) reached 0.017 mg/L, 0.021 mg/L and 0.027 mg/L of Ti (mean values; Table S1), respectively. On the other hand, results from ZnO NPs dissolution showed that the concentrations of releasing Zn gradually increased with increasing concentrations. The concentration of Zn dissolved from ZnO NPs suspensions ranged from 1.22 mg/L (10 mg/L ZnO NPs) to 10.57 mg/L (300 mg/L ZnO NPs). Also, releasing of Cr gradually increased with increasing $K_2Cr_2O_7$ concentrations. Average values of Cr ranged from 1.12 mg/L (3.2 mg/L $K_2Cr_2O_7$) to 17.5 mg/L (50 mg/L $K_2Cr_2O_7$) (Table S1). Since the measured concentrations of PEG were nearly equal to the nominal concentrations (Table S1), we reported all the results based on the latter.

2.10. Growth inhibition tests

Table 1 presents the results of the inhibition growth test, growth rate and the related EC_{50}. The EC_{50} of $K_2Cr_2O_7$ was around 20 mg/L in both species: 22.97 ± 1.34 mg/L in *P. tricornutum* and 19.84 ± 1.45 mg/L in *C. tenuissimus*. The EC_{50} of TiO_2 was 75.15 ± 2.16 mg/L for *P. tricornutum*, while that for *C. tenuissimus* was estimated at 57.02 ± 2.23 mg/L. The EC_{50} of n-ZnO in *P. tricornutum* was 32.48 ± 1.99 mg/L, higher than the 13.15 ± 1.10 mg/L measured in *C. tenuissimus*. Lastly, the EC_{50} of PEG was 100.73 ± 2.32 mg/L in *P. tricornutum* and 52.01 ± 1.76 mg/L in *C. tenuissimus*.

2.11. Biochemical analyses

Table 2 presents the concentrations (mg/m^3) of the biochemical biomarkers (Chl *a, c*) in the two microalgal species exposed to the four chemicals. Kruskal–Wallis test revealed significant difference between the treatments and control groups ($p < 0.05$). Generally, Chl-*a* concentrations were always significantly higher in negative controls compared to both *P. tricornutum* and *C. tenuissimus* exposed to the four chemicals (Dunn's test, $p < 0.05$). On the other hand, the Chl-*c* concentrations were almost always undetectable (<LOQ) in both the microalgae species exposed to the four chemicals, except at the lowest concentrations of $K_2Cr_2O_7$, n-ZnO and PEG.

Table 1
Inhibition of growth (%), growth rate (μ), and estimated EC_{50} (mg/L) in *P. tricornutum* and *C. tenuissimus* after 72 h of exposure to $K_2Cr_2O_7$, n-TiO_2, n-ZnO and polyethylene glycol (PEG). SD = standard deviation.

Chemical	Concentration (mg/L)	Inhibition (%)		Growth rate (μ)		EC_{50} ± SD (mg/L)	
		P. tricornutum	*C. tenuissimus*	*P. tricornutum*	*C. tenuissimus*	*P. tricornutum*	*C. tenuissimus*
$K_2Cr_2O_7$	50	100	100	0	0	22.97 ± 1.34	19.84 ± 1.45
	32	96.32	100	0.009	0		
	18	27.22	29.64	0.058	0.051		
	10	22.51	18.48	0.062	0.059		
	5.6	13.70	3.68	0.075	0.069		
	3.2	6.61	3.92	0.074	0.071		
n-TiO_2	300	100	100	0	0	75.15 ± 2.16	57.02 ± 2.23
	200	100	100	0	0		
	100	72.94	72.09	0.022	0.022		
	50	47.96	60.14	0.042	0.033		
	25	43.20	20.34	0.045	0.067		
	10	38.33	13.23	0.049	0.072		
n-ZnO	300	100	100	0	0	32.48 ± 1.99	13.15 ± 1.10
	200	100	100	0	0		
	100	100	100	0	0		
	50	100	100	0	0		
	25	53.64	96.33	0.034	0.009		
	10	44.83	36.76	0.04	0.051		
PEG	500	100	100	0	0	100.73 ± 2.32	52.01 ± 1.76
	250	100	100	0	0		
	100	48.53	74.68	0.037	0.02		
	50	−18.48	63.06	0.086	0.029		
	25	−8.12	26.66	0.079	0.059		
	10	−1.31	15.49	0.074	0.068		

Table 2
Biochemical quantification of chlorophyll (Chl-*a*, Chl-*c*) in *C. tenuissimus* and *P. tricornutum* after 72 h exposure to $K_2Cr_2O_7$, TiO_2, ZnO and polyethylene glycol (PEG). Measurements are expressed in mg/m^3. LOQ = limit of quantification. Lower case letters denote significant difference ($p < 0.05$) between exposed microalgae cultures and negative controls disclosed by Dunn's post-hoc test.

Chemical	Concentration (mg/L)	Chl-*a* *P. tricornutum*	*C. tenuissimus*	Chl-*c* *P. tricornutum*	*C. tenuissimus*
Negative Control	–	0.323 ± 0.003^a	0.128 ± 0.004^a	0.020 ± 0.002^a	0.030 ± 0.003^a
$K_2Cr_2O_7$	50	0.049 ± 0.002^b	0.031 ± 0.005^b	<LOQ	<LOQ
	32	0.091 ± 0.003^b	0.039 ± 0.005^b	<LOQ	<LOQ
	18	0.174 ± 0.004^b	0.048 ± 0.004^b	<LOQ	<LOQ
	10	0.189 ± 0.007^b	0.056 ± 0.007^b	<LOQ	<LOQ
	5.6	0.200 ± 0.001^b	0.078 ± 0.005^b	0.026 ± 0.003^a	0.023 ± 0.002^a
	3.2	0.210 ± 0.012^b	0.087 ± 0.002^b	0.016 ± 0.005^a	0.026 ± 0.006^a
n-TiO_2	300	0.042 ± 0.007^b	0.019 ± 0.002^b	<LOQ	<LOQ
	200	0.057 ± 0.010^b	0.025 ± 0.002^b	<LOQ	<LOQ
	100	0.060 ± 0.009^b	0.035 ± 0.003^b	<LOQ	<LOQ
	50	0.100 ± 0.013^b	0.042 ± 0.006^b	<LOQ	<LOQ
	25	0.157 ± 0.008^b	0.051 ± 0.004^b	<LOQ	<LOQ
	10	0.210 ± 0.006^b	0.088 ± 0.005^b	<LOQ	<LOQ
n-ZnO	300	0.038 ± 0.002^b	0.018 ± 0.002^b	<LOQ	<LOQ
	200	0.052 ± 0.002^b	0.026 ± 0.005^b	<LOQ	<LOQ
	100	0.059 ± 0.003^b	0.038 ± 0.002^b	<LOQ	<LOQ
	50	0.112 ± 0.005^b	0.049 ± 0.005^b	<LOQ	<LOQ
	25	0.143 ± 0.004^b	0.058 ± 0.006^b	0.001 ± 0.001^b	0.004 ± 0.002^b
	10	0.177 ± 0.005^b	0.092 ± 0.003^b	0.007 ± 0.001^b	0.008 ± 0.001^b
PEG	500	0.050 ± 0.003^b	0.018 ± 0.002^b	<LOQ	<LOQ
	250	0.047 ± 0.002^b	0.038 ± 0.002^b	<LOQ	<LOQ
	100	0.055 ± 0.002^b	0.043 ± 0.006^b	<LOQ	<LOQ
	50	0.248 ± 0.003^b	0.051 ± 0.007^b	<LOQ	<LOQ
	25	0.297 ± 0.002^b	0.059 ± 0.015^b	0.018 ± 0.004^a	0.028 ± 0.001^a
	10	0.299 ± 0.009^b	0.102 ± 0.007^b	0.019 ± 0.005^a	0.029 ± 0.001^a

Table 3 presents the EC_{50} (toxicant concentration that produces a decrease of 50% in biomarker concentration in the exposed cells compared against the concentration in the negative controls) calculated on the percentage (%) of change in the Chl-*a* and Chl-*c* concentration in the exposed cultures compared to negative controls. The EC_{50} of $K_2Cr_2O_7$ was lower in *C. tenuissimus* (8.89 ± 1.01 mg/L) and higher in *P. tricornutum* (9.46 ± 1.23 mg/L). The EC_{50} of n-TiO_2 in *P. tricornutum* was 14.21 ± 1.56 mg/L and 13.15 ± 1.23 mg/L in *C. tenuissimus*; the EC_{50} of n-ZnO was 19.52 ± 1.78 mg/L in *P. tricornutum* and 17.27 ± 1.65 mg/L in *C. tenuissimus*. Finally, the EC_{50} of PEG was 67.79 ± 2.02 mg/L in *P. tricornutum* and 18.51 ± 1.98 mg/L in *C. tenuissimus*. The EC_{50} values calculated on inhibition of Chl-*c* were not reported in either species (concentrations < LOQ).

Table 4 presents the Chl-*a* and Chl-*c* concentrations estimated at the EC_{50} (algal growth inhibition). Generally, there was a significant difference in both species at the EC_{50} for all chemicals in the exposed cultures compared to the negative controls (Kruskal–Wallis test, $p < 0.05$). Dunn's test revealed a significant difference ($p < 0.05$) between negative controls and treatments for all chemicals in both species.

Table 3
EC_{50} (mg/L) calculated on inhibition of chlorophyll (Chl-*a*, Chl-*c*) concentrations. EC_{50} in biomarkers was calculated from the percentage effect of exposed culture and negative controls. NC = not calculable.

Test	Chemical	EC_{50}		P. tricornutum	C. tenuissimus
Biochemical analyses (Chlorophylls)	Chl-a	$K_2Cr_2O_7$	mg/L	9.46 ± 1.23	8.89 ± 1.01
		n-TiO_2	mg/L	14.21 ± 1.56	13.15 ± 1.23
		n-ZnO	mg/L	19.52 ± 1.78	17.27 ± 1.65
		PEG	mg/L	67.79 ± 2.02	18.51 ± 1.98
	Chl-c	$K_2Cr_2O_7$	mg/L	NC	NC
		n-TiO_2	mg/L	NC	NC
		n-ZnO	mg/L	NC	NC
		PEG	mg/L	NC	NC

2.12. Molecular changes in chlorophyll

Two examples of the spectra overlay between the exposed cultures and the negative control are reported in Fig. 1.

Table 5 presents the mean spectral match (%) between the spectra of the exposed cultures compared against the negative controls (100% denotes identity with the negative controls). The whole spectrum responses exhibited a range of alterations from 90.68% to 98.22%, with the lower matches were associated with PEG exposure in both species.

Table 6 presents the mean regional spectral match of each of the nine visible peaks. The results refer to the EC_{50} of each chemical tested in the two species. The infrared spectrum regions exhibited a broader range of alteration, with matches ranged from 61.99% to 99.61% for *P. tricornutum* and from 15.21% to 99.27% for *C. tenuissimus*. The lower limit was associated with regions 1 (675 – 771 cm^{-1}), 7 (2307 – 2411 cm^{-1}), 8 (2831 – 3066 cm^{-1}), and 9 (3225 – 3741 cm^{-1}) of the spectrum, generally for all chemicals and major alterations after exposure to PEG.

Principal component analysis performed on the whole IR spectrum disclosed changes in absorbance of the photosynthetic complex after exposure to the chemicals. The first PCA plot (Fig. 2a) showed that the first (F1) component, and some of the second (F2), generated a total variance of 99.65% (97.46 and 2.18%, respectively). It is possible to observe the changes in spectral response generated by the four chemicals in both microalgal species. There was a similar but not identical trend in spectral response, as confirmed by the overlap of the confidence ellipses of all chemicals; however, it is possible to highlight how spectra from microalgae exposed to PEG, n-ZnO and n-TiO_2 showed higher variability (see confidence ellipses), indicating a certain level of molecular change compared to negative controls (see Table 5). The second PCA (Fig. 2a) showed how group C (*C. tenuissimus*) was almost totally included in the space of the group P (*P. tricornutum*), indicating changes

Table 4
Estimated chlorophyll (Chl-*a*, Chl-*c*) concentration (mg/m^3) at EC_{50}. Lower case letters denote significant difference ($p < 0.05$) between exposed microalgae cultures and negative controls disclosed by Dunn's post-hoc test. LOQ = limit of quantification.

Test	Chemical	Concentration	P. tricornutum	C. tenuissimus	
Biochemical analyses (Chlorophylls)	Chl-a	Negative Control	mg/m^3	0.323 ± 0.003^a	0.118 ± 0.004^a
		$K_2Cr_2O_7$	mg/m^3	0.192 ± 0.005^b	0.086 ± 0.003^b
		n-TiO_2	mg/m^3	0.187 ± 0.004^b	0.075 ± 0.002^b
		n-ZnO	mg/m^3	0.151 ± 0.002^b	0.069 ± 0.004^b
		PEG	mg/m^3	0.175 ± 0.006^b	0.064 ± 0.007^b
	Chl-c	Negative Control	mg/m^3	0.020 ± 0.002	0.030 ± 0.003
		$K_2Cr_2O_7$	mg/m^3	<LOQ	<LOQ
		n-TiO_2	mg/m^3	<LOQ	<LOQ
		n-ZnO	mg/m^3	<LOQ	<LOQ
		PEG	mg/m^3	<LOQ	<LOQ

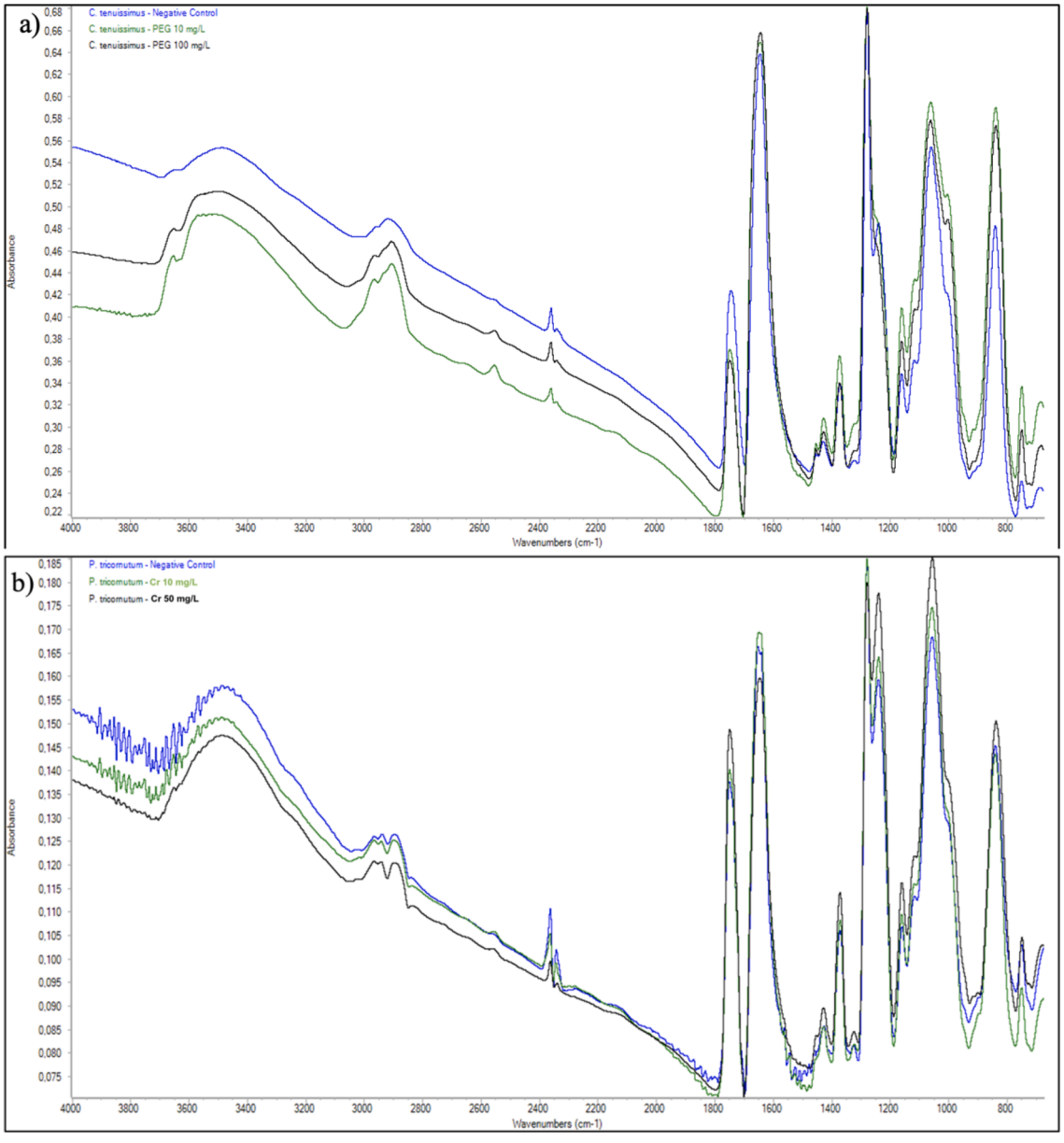

Fig. 1. Molecular changes revealed by μFT-IR. Example of average spectra overlay on *C. tenuissimus* (a) exposed to PEG at concentrations of 10 mg/L (green) and 100 mg/L (black) compared to negative control (blue) and *P. tricornutum* (b) exposed to n-TiO_2 at concentrations of 10 mg/L (green) and 50 mg/L (black) compared to negative control (blue).

Table 5
Mean percentage of spectral match between spectra of exposed cell cultures (n = 10) and negative controls (n = 10). Matches were recorded at exposure to EC_{50}. Data refer to the whole spectral response. 100% denotes identity with the negative controls.

Chemical	*P. tricornutum* (%)	*C. tenuissimus* (%)
$K_2Cr_2O_7$	98.22	94.28
n-TiO_2	96.24	92.76
n-ZnO	95.01	94.18
PEG	93.40	90.68

Table 6
Matches (in percentage; %) of the 9 infrared spectrum regions (visible peaks) between average spectra of exposed cultures (EC_{50}) and negative controls. 100% denotes total correlation.

velength group	Spectral range (cm^{-1})	Chemical	Match (%) *P. tricornutum*	*C. tenuissimus*
1	675–771	$K_2Cr_2O_7$	99.61	93.83
		n-TiO_2	97.31	94.86
		n-ZnO	99.07	85.41
		PEG	99.5	95.84
2	775–937	$K_2Cr_2O_7$	99.04	97.62
		n-TiO_2	96.03	97.67
		n-ZnO	97.05	97.34
		PEG	96.76	97.92
3	937–1188	$K_2Cr_2O_7$	99.37	99.27
		n-TiO_2	97.44	97.34
		n-ZnO	98.18	98.32
		PEG	95.37	97.13
4	1192–1331	$K_2Cr_2O_7$	98.65	97.72
		n-TiO_2	96.7	98.56
		n-ZnO	96.03	98.72
		PEG	94.27	96.12
5	1342–1481	$K_2Cr_2O_7$	99	97.85
		n-TiO_2	99.43	95.65
		n-ZnO	99.19	97.7
		PEG	97.94	96.74
6	1504–1813	$K_2Cr_2O_7$	97.99	96.9
		n-TiO_2	96.48	94.63
		n-ZnO	95.07	96.67
		PEG	92.56	94.43
7	2307–2411	$K_2Cr_2O_7$	96.89	87.06
		n-TiO_2	98.99	72.91
		n-ZnO	74.19	72.6
		PEG	99.05	24.57
8	2831–3066	$K_2Cr_2O_7$	85.76	94.65
		n-TiO_2	61.99	83.87
		n-ZnO	62.42	89.65
		PEG	83.67	96.42
9	3225–3741	$K_2Cr_2O_7$	85.94	55.72
		n-TiO_2	90.37	15.21
		n-ZnO	79.68	41.49
		PEG	75.12	23.9

in spectral response in both species exposed to chemicals; this condition was confirmed by the overlap of the confidence ellipses (95%) of each one. However, the range values of spectral mismatch from *C. tenuissimus* (90.68–94.28%; Table 5) are more homogeneous than those obtained from *P. tricornutum* (range: 93.40–98.22%; Table 5) exposed to chemicals.

3. Discussion

The vulnerability of microalgae to pollutants is influenced by several factors, including cell size, cell wall type and thickness, and taxonomic group features (Tato and Beiras, 2019). Small cells have a high surface area to volume ratio, which increases their solute uptake rates and, as a result, their sensitivity to contaminants (Tato and Beiras, 2019). On this path, *Chaetoceros tenuissimus* is rectangular in the girdle view and is one

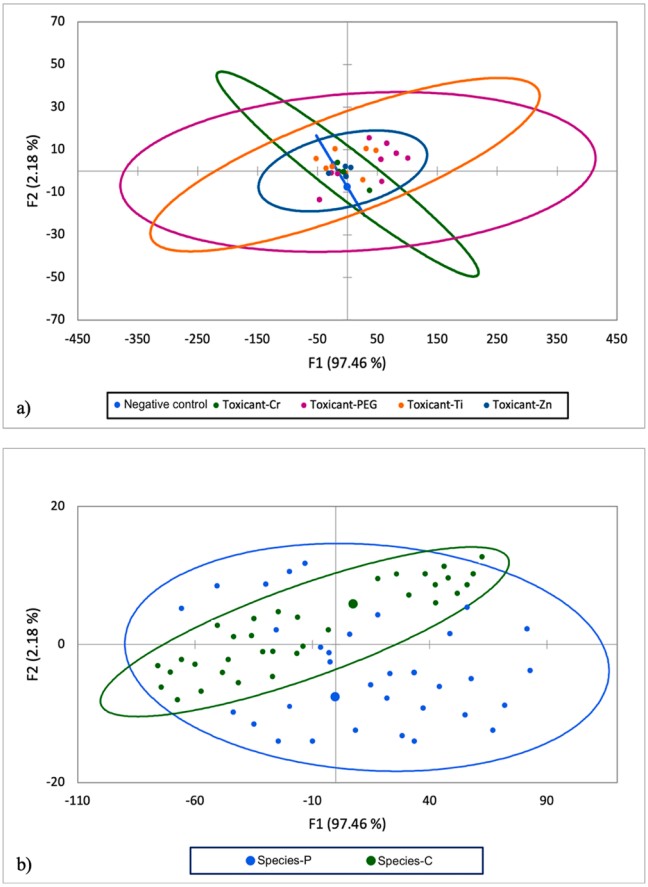

Fig. 2. Principal component analysis of spectra (obtained by μFT-IR) with confidence ellipses (95%). a) Clusters grouped by exposed (Cr denotes $K_2Cr_2O_7$; Ti n-TiO_2; Zn n-ZnO; PEG polyethylene glycol) and untreated algal cultures (N denotes negative control); b) clusters of the two phytoplankton species: C denotes *Chaetoceros tenuissimus;* P *Phaeodactylum tricornutum*; larger dots denote negative controls.

of the smallest (~5 μm) diatoms, explaining its higher sensitivity to the four chemicals compared to *P. tricornutum* (~15 μm in size). Such finding was also reported by Quigg et al. (2006) which showed a higher Cu uptake by *Synechococcus* sp. compared to other algal species (i.e., *Pryamimonas parkeae*, *Amphidinum carterae*, *Emiliania huxleyi*, *Thalassiosira seudonana* and *T. weissflogii*) due to its largest cell surface-to-volume ratio.

Generally, the effects of the four chemicals were greater for *C. tenuissimus* (more sensitive). Indeed, we observed a lower EC_{50} for growth inhibition test after exposure to chemicals in *C. tenuissimus* than *P. tricornutum*. For the first time, here we have defined the EC_{50} values for $K_2Cr_2O_7$, n-ZnO, n-TiO_2 and PEG in *C. tenuissimus*. Thus, it was not possible to make comparisons with literature. On the other hand, the EC_{50} of $K_2Cr_2O_7$ for *P. tricornutum* was in line with the ISO procedures (ISO, 2017) and with the value (16.21 ± 1.72 mg/L) reported by Piccardo et al. (2021). The EC_{50} of n-ZnO in *P. tricornutum* was in line with values reported by Broccoli et al. (2021) (20.36 mg/L). The EC_{50} of n-TiO_2 was also in line with value (72.70 mg/L) reported by Wang et al. (2016).

Heavy metals (e.g., Cr, Zn, Ti) compounds are highly toxic to living organisms, and those considered as essential can be toxic when present in high concentration (Mudgal et al., 2010). The mechanism of toxicity of metals is not always clear (Pinto et al., 2003), since it may depend on the type of the pollutant and its concentration (Gupta and Singh, 2011). Heavy metals ions can interact with many cell components, such as DNA and nuclear proteins, causing DNA damage and conformational changes

that can alter cell-cycle modulation and induce apoptosis (Chang et al., 1996; Beyersmann and Hartwig, 2008). In this study, we observed how solubility of TiO_2 NPs was quite low, being the Ti concentrations in algal medium almost below the LOQ. On this path, Joonas et al. (2019) and Wu et al. (2019) also found how TiO_2 NPs (although sonication) did not solubilize in algal medium, and it could be inferred that the effects of TiO_2 NPs were in part due to the heteroagglomeration between NPs and microalgae. On the other hand, dissolution of Zn is an important factor in ZnO NP ecotoxicity and has been extensively demonstrated in the literature (Chen et al., 2014). Our data demonstrates that ZnO NP were dissolved in the algal medium used in this study, and the extent of Zn dissolution was comparable with previous ZnO NPs algal toxicity studies (Suman et al., 2015; Oukarroum et al., 2019). It is well documented that high concentrations of ZnO NPs can cause significant toxic effects with significant changes in morphology of the algae cells (Pereira et al., 2020).

For the first time, here we have also defined the EC_{50} value for PEG in both species, which was higher than for the other chemicals. Despite the wide application of this chemical, very few studied assess the negative effects on biota (Nascimento et al., 2021), and we know nothing about the impact of PEG on phytoplankton. As regard the mechanisms of toxicity, Tato and Beiras (2019) highlighted that generally, the thickness of the cell wall represents a key factor to explain the damage caused by surfactants to microalgae. Pérez et al. (2009) also found discrepancies in the toxicity response to surfactants in *Isochrysis galbana* and *C. gracilis* due to their differences in cell wall structure.

Photosynthesis is known to be reduced in presence of contaminants (Yang et al., 2021). Thus, chlorophyll-*a* and chlorophyll-*c* contents were utilized as a measure of physiological stress (Monni et al., 2001). Microalgal species here tested showed a significant drop in chlorophyll-*a* content, implying a change in photosynthetic activity. Moreover, EC_{50} values calculated on the inhibition of Chl-*a* concentrations were lower for all chemicals compared to those obtained from the growth inhibition tests. Such findings suggest that Chl-*a* represents an earlier endpoint than the responses obtained in the standardized algal growth inhibition tests. Therefore, the decrease in Chl-*a* concentrations represents a key indicator for assessing the impact of environmental contaminants. Chlorophyll-*c* content was also investigated. However, in the exposed microalgae the values were almost lower than the LOQ compared to the negative controls, suggesting a non-use of Chl-*c* as ecotoxicological endpoint. Indeed, the Chl-*c* represent only a minor component of the fucoxanthin-chlorophyll protein (FCP) which is the key molecular complex performing the light-harvesting function in diatoms (Kuczynska et al., 2015).

In this study, differences in molecular change between the cultures exposed at EC_{50} and the negative controls were also reported, as demonstrated by the spectrum match. This kind of analysis proved to be a powerful tool to discriminate premature alterations in the molecule structure composing the phytoplankton cells. For both species, $K_2Cr_2O_7$ exhibited the least spectrum alteration, while PEG demonstrated the greatest. In general, chemical exposure generated a stronger spectrum alteration in *C. tenuissimus* than in *P. tricornutum*, confirming the greater effects of the four chemicals on the unstandardized *C. tenuissimus*, in line with the algal growth inhibition and Chl-*a* endpoints. Principal component analysis graphically highlighted such molecular changes, also suggesting that *C. tenuissimus* has a less variability in the spectral match rage alterations (90–94%) than the standardized *P. tricornutum* (range: 93–98%).

Region changes in IR spectra are an important means to discriminate the kind of damage on chlorophyll structure (Broccoli et al., 2021): changes in the IR spectra in the range of about 3500 cm^{-1} observed in both species were associated with OH stretching due to alteration in carbohydrates, proteins, lipids (sterols and fatty acids). Alterations in regions of about 2950 cm^{-1}, observed in both species, were associated with CH_3 stretching caused by lipids and proteins and protein damage. Furthermore, relevant alterations observed only in *P. tricornutum* occurred in regions of about 697–753 cm^{-1} were associated with CH_2 bending on carbohydrates, proteins, lipids (Mecozzi et al., 2008). Lastly, we observed relevant alterations in the spectral region of 2307–2411 cm^{-1} in both species.

The multidisciplinary approach (growth inhibition, biochemical and infrared spectroscopy analyses) here tested suggests that *C. tenuissimus* could be particularly adapted to ecotoxicity testing in samples from marine ecosystems being quite common in the brackish and marine water of fiords and inlets.

4. Conclusions

In this study we characterized by growth inhibition, biochemical and infrared spectroscopy analyses the diatom *Chaetoceros tenuissimus* exposed to four CECs in comparison to the standardized *P. tricornutum*. The sensitivity of *C. tenuissimus* was almost higher than the standardized species (*P. tricornutum*) for both inhibitions of growth and chlorophyll-a concentrations endpoints. This emphasizes that careful consideration should be given in data extrapolation to the whole trophic level.

Considering that *C. tenuissimus* is easy to culture and has a widespread distribution the marine and coastal environment, it represents a valid alternative to the standardized *P. tricornutum* especially in water contaminated by $K_2Cr_2O_7$, n-ZnO, n-TiO_2 and PEG. Furthermore, this study adds a step of knowledge on the behaviour of CECs on phytoplankton species, useful to understand their mechanisms on organisms at higher trophic levels and on the whole aquatic environment. Further studies are needed to better understand the microalgal species sensitiveness to other contaminants.

CRediT authorship contribution statement

Paolo Pastorino: Conceptualization, Data curation, Investigation, Methodology, Writing – original draft, Writing – review & editing. **Andrea Broccoli:** Investigation, Conceptualization, Methodology, Writing – original draft. **Serena Anselmi:** Investigation, Methodology, Writing – review & editing. **Elisa Bagolin:** Investigation, Methodology, Writing – review & editing. **Marino Prearo:** Conceptualization, Methodology, Writing – review & editing. **Damià Barceló:** Conceptualization, Methodology, Writing – review & editing. **Monia Renzi:** Conceptualization, Investigation, Methodology, Supervision, Writing – review & editing.

Declaration of Competing Interest

The authors declare that they have no known competing financial interests or personal relationships that could have appeared to influence the work reported in this paper.

Data availability

Data will be made available on request.

Appendix A. Supplementary data

Supplementary data to this article can be found online at https://doi.org/10.1016/j.ecolind.2022.109075.

References

Agathokleous, E., Barceló, D., Fatta-Kassinos, D., Moore, M.N., Calabrese, E.J., 2021. Contaminants of emerging concern and aquatic organisms: the need to consider hormetic responses in effect evaluations. Water Emerging Contaminants & Nanoplastics 1 (1), 2.

Aravantinou, A.F., Tsarpali, V., Dailianis, S., Manariotis, I.D., 2015. Effect of cultivation media on the toxicity of ZnO nanoparticles to freshwater and marine microalgae. Ecotoxicology and environmental safety 114, 109–116.

APAT, Cnr, IRSA., 2003. Metodologie analitiche per il controllo della qualità delle acque. Manuali e Linee guida, Par, p. 9020.

Beleites, C., Steiner, G., Sowa, M.G., Baumgartner, R., Sobottka, S., Schackert, G., Salzer, R., 2005. Classification of human gliomas by infrared imaging spectroscopy and chemometric image processing. Vib. Spectroscopy 38 (1-2), 143–149.
Benjamin, L.V., Kutty, R., 2019. Sub-lethal effects of potassium dichromate on hematological and histological parameters in climbing perch, *Anabas testudineus* (Anabantidae). International Journal of Aquatic Biology 7 (3), 140–145.
Besha, A.T., Liu, Y., Fang, C., Bekele, D.N., Naidu, R., 2020. Assessing the interactions between micropollutants and nanoparticles in engineered and natural aquatic environments. Critical Reviews in Environmental Science and Technology 50 (2), 135–215.
Beyersmann, D., Hartwig, A., 2008. Carcinogenic metal compounds: recent insight into molecular and cellular mechanisms. Archives of Toxicology 82 (8), 493–512.
Broccoli, A., Anselmi, S., Cavallo, A., Ferrari, V., Prevedelli, D., Pastorino, P., Renzi, M., 2021. Ecotoxicological effects of new generation pollutants (nanoparticles, amoxicillin and white musk) on freshwater and marine phytoplankton species. Chemosphere 279, 130623.
Chang, L.W., Magos, L., Suzuki, T., 1996. Toxicology of metals. CRC, Boca Raton, FL.
Chen, T.H., Lin, C.C., Meng, P.J., 2014. Zinc oxide nanoparticles alter hatching and larval locomotor activity in zebrafish (*Danio rerio*). Journal of hazardous materials 277, 134–140.
Deasi, S.R., Verlecar, X.N., Ansari, Z.A., Jagtap, T.G., Sarkar, A., Vashistha, D., Dalal, S. G., 2010. Evaluation of genotoxic responses of *Chaetoceros tenuissimus* and *Skeletonema costatum* to water accommodated fraction of petroleum hydrocarbons as biomarker of exposure. Water Research 44 (7), 2235–2244.
Desai, S.R., Verlecar, X.N., Nagarajappa, U., G.,, 2006. Genotoxicity of cadmium in marine diatom *Chaetoceros tenuissimus* using the alkaline Comet assay. Ecotoxicology 15, 359–363.
Epa, 1991. Method 600/4-90-027. Methods for Measuring the Acute Toxicity of Effluents and Receiving Waters to Freshwater and Marine Organisms, 4th ed. Cincinnati, USA.
Fleeger, J.W., Carman, K.R., Nisbet, R.M., 2003. Indirect effects of contaminants in aquatic ecosystems. Science of the Total Environment 317 (1–3), 207–233.
Gomaa, M., Zien-Elabdeen, A., Hifney, A.F., Adam, M.S., 2021. Environmental risk analysis of pharmaceuticals on freshwater phytoplankton assemblage: effects on alpha, beta, and taxonomic diversity. Environmental Science and Pollution Research 28 (8), 9954–9964.
Gupta, S.K., Singh, J., 2011. Evaluation of mollusc as sensitive indicator of heavy metal pollution in aquatic system: a review. IIOAB Journal 2 (1), 49–57.
Häder, D.P., Gao, K., 2015. Interactions of anthropogenic stress factors on marine phytoplankton. Frontiers in Environmental Science 3, 14.
Hano, T., Tomaru, Y., 2019. Metabolomics-based approach to explore growth phase-dependent markers in cultured diatom *Chaetoceros tenuissimus*. Journal of Chromatography B 1128, 121779.
Hongo, Y., Kimura, K., Takaki, Y., Yoshida, Y., Baba, S., Kobayashi, G., Nagasaki, K., Hano, T., Tomaru, Y., 2021. The genome of the diatom *Chaetoceros tenuissimus* carries an ancient integrated fragment of an extant virus. Scientific reports 11 (1).
Iso, 2016. UNI EN ISO 10253:2016. Water Quality—Marine Algal Growth Inhibition Test with *Skeletonema* sp. and *Phaeodactylum tricornutum*. accessed on 20 January 2021 Available online. https://www.iso.org/standard/66657.html.
Iso, 2017. UNI EN ISO 10253:2017. Water quality, marine algal growth inhibition test with *Skeletonema* sp. and *Phaeodactylum tricornutum* accessed on 20 January 2021.
ISO, 2018. UNI CEI EN ISO/IEC 17025:2018. General requirements for the competence of testing and calibration laboratories. http://store.uni.com/catalogo/uni-cei-en-iso-iec-17025-2018?josso_back_to=http://store.uni.com/josso-security-check.php&josso_cmd=login_optional&josso_partnerapp_host=store.uni.com (accessed on 20 January 2021).
Jang, H.J., Shin, C.Y., Kim, K.B., 2015. Safety Evaluation of Polyethylene Glycol (PEG) Compounds for Cosmetic Use. Toxicological Research 31 (2), 105–136.
Joonas, E., Aruoja, V., Olli, K., Kahru, A., 2019. Environmental safety data on CuO and TiO_2 nanoparticles for multiple algal species in natural water: filling the data gaps for risk assessment. Science of the total environment 647, 973–980.
Krull, M., Barros, F., 2012. Key issues in aquatic ecotoxicology in Brazil: a critical review. Ecotoxicology and Environmental Contamination 7 (2), 57–66.
Kuczynska, P., Jemiola-Rzeminska, M., Strzalka, K., 2015. Photosynthetic Pigments in Diatoms. Marine Drugs 13 (9), 5847–5881. https://doi.org/10.3390/md13095847.
Labra, M., Bernasconi, M., Grassi, F., De Mattia, F., Sgorbati, S., Airoldi, R., Citterio, S., 2007. Toxic and genotoxic effects of potassium dichromate in *Pseudokirchneriella subcapitata* detected by microscopy and AFLP marker analysis. Aquatic botany 86 (3), 229–235.
Lawrence, M.J., 1994. Surfactant systems: their use in drug delivery. Chemical Society Reviews 23, 417–424.
Levy, J.L., Stauber, J.L., Jolley, D.F., 2007. Sensitivity of marine microalgae to copper: the effect of biotic factors on copper adsorption and toxicity. Science of the Total Environment 387 (1-3), 141–154.
Li, Y., Meng, J., Zhang, C., Ji, S., Kong, Q., Wang, R., Liu, J., Guo, X., 2020. Bottom-up and top-down effects on phytoplankton communities in two freshwater lakes. PLoS ONE 15 (4), e0231357.
Luan, X., Liu, X., Fang, C., Chu, W., Xu, Z., 2020. Ecotoxicological effects of disinfected wastewater effluents: a short review of in vivo toxicity bioassays on aquatic organisms. Environmental Science: Water Research & Technology 6 (9), 2275–2286.
McCormick, P.V., Cairns, J., 1994. Algae as indicators of environmental change. Journal of Applied Phycology 6 (5-6), 509–526.
McPherson, C.A., Chapman, P.M., 2000. Copper effects on potential sediment test organisms: the importance of appropriate sensitivity. Marine Pollution Bulletin 40 (8), 656–665.
Mecozzi, M., Onorati, F., Oteri, F., Sarni, A., 2008. Characterisation of a bioassay using the marine alga *Dunaliella tertiolecta* associated with spectroscopic (visible and infrared) detection. International Journal of Environment and Pollution 32 (1), 104–120.
Monni, S., Uhlig, C., Hansen, E., Magel, E., 2001. Ecophysiological responses of Empetrum nigrum to heavy metal pollution. Environmental Pollution 112 (2), 121–129.
Mucha, A.P., Leal, M.F.C., Bordalo, A.A., Vasconcelos, M.T.S.D., 2003. Comparison of the response of three microalgae species exposed to elutriates of estuarine sediments based on growth and chemical speciation. Environmental Toxicology and Chemistry: An international Journal 22 (3), 576–585.
Mudgal, V., Madaan, N., Mudgal, A., Singh, R.B., Mishra, S., 2010. Effect of Toxic Metals on Human Health. The Open Nutraceuticals Journal 3 (1), 94–99.
Nascimento, Í.F., Guimarães, A.T.B., Ribeiro, F., Rodrigues, A.S.d.L., Estrela, F.N., Luz, T. M.d., Malafaia, G., 2021. Polyethylene glycol acute and sub-lethal toxicity in neotropical *Physalaemus cuvieri* tadpoles (Anura, Leptodactylidae). Environmental Pollution 283, 117054.
OECD, 2000. OECD Economic Surveys: Mexico 1999/2000, Vol. 2000, Issue 13.
Oecd, 2011. OECD Guidelines for the Testing of Chemicals. Freshwater Alga and Cyanobacteria, Growth Inhibition Test No. 201".
Oukarroum, A., Halimi, I., Siaj, M., 2019. Cellular responses of *Chlorococcum* sp. Algae exposed to Zinc oxide nanoparticles by using flow cytometry. Water, Air, & Soil Pollution 230 (1), 1.
Parmar, T.K., Rawtani, D., Agrawal, Y.K., 2016. Bioindicators: the natural indicator of environmental pollution. Frontiers in life science 9 (2), 110–118.
Pastorino, P., Broccoli, A., Bagolin, E., Anselmi, S., Cavallo, A., Prearo, M., Renzi, M., 2021. A Multidisciplinary Approach to Evaluate the Effects of Contaminants of Emerging Concern on Natural Freshwater and Brackish Water Phytoplankton Communities. Biology 10 (10), 1039.
Pastorino, P., Ginebreda, A., 2021. Contaminants of Emerging Concern (CECs): Occurrence and Fate in Aquatic Ecosystems. International journal of environmental research and public health 18 (24), 13401.
Pereira, F.F., Paris, E.C., Bresolin, J.D., Mitsuyuki, M.C., Ferreira, M.D., Corrêa, D.S., 2020. The effect of ZnO nanoparticles morphology on the toxicity towards microalgae *Pseudokirchneriella subcapitata*. Journal of Nanoscience and Nanotechnology 20 (1), 48–63.
Pérez, P., Fernández, E., Beiras, R., 2009. Toxicity of benzalkonium chloride on monoalgal cultures and natural assemblages of marine phytoplankton. Water Air Soil Pollut. 201 (1-4), 319–330.
Puiseux-Dao, S., 2018. Phytoplankton Model in Ecotoxicology. In: Aquatic Ecotoxicology: Fundamental Concepts and Methodologies. CRC Press, pp. 163–186.
Piccardo, M., Provenza, F., Grazioli, E., Anselmi, S., Terlizzi, A., Renzi, M., 2021. Impacts of Plastic-Made Packaging on Marine Key Species: Effects Following Water Acidification and Ecological Implications. J. Mar. Sci. Eng. 2021 (9), 432.
Pinto, E., Sigaud-Kutner, C.S.T., Zajac, M.A., Okamoto, O., Morse, D., Colepicolo, P., 2003. Heavy metal-induced oxidative stress in algae. Journal of Phycology 39, 1008–1018.
Prajitha, N., Athira, S.S., Mohanan, P.V., 2019. Bio-interactions and risks of engineered nanoparticles. Environmental research 172, 98–108.
Quigg, A., Reinfelder, J.R., Fisher, N.S., 2006. Copper uptake kinetics in diverse marine phytoplankton. Limnology and oceanography 51 (2), 893–899.
Rao, K., Zhang, X., Yi, X.J., Li, Z.S., Wang, P., Huang, G.W., Guo, X.X., 2018. Interactive effects of environmental factors on phytoplankton communities and benthic nutrient interactions in a shallow lake and adjoining rivers in China. Science of the Total Environment 619, 1661–1672.
Renzi, M., Blašković, A., 2019. Ecotoxicity of nano-metal oxides: A case study on Daphnia magna. Ecotoxicology 28 (8), 878–889.
Renzi, M., Guerranti, C., 2015. Ecotoxicity of nanoparticles in aquatic environments: a review based on multivariate statistics of meta- data. International Journal of Environmental Analytical Chemistry 2 (4), 149.
Renzi, M., Roselli, L., Giovani, A., Focardi, S.E., Basset, A., 2014. Early warning tools for ecotoxicity assessment based on *Phaeodactylum tricornutum*. Ecotoxicology 23 (6), 1055–1072.
Rodrigues, S., Pinto, I., Formigo, N., Antunes, S.C., 2021. Microalgae Growth Inhibition-Based Reservoirs Water Quality Assessment to Identify Ecotoxicological Risks. Water 13 (19), 2605.
Sarker, S., Desai, S.R., Verlecar, X.N., Saha Sarker, M., Sarkar, A., 2016. Mercury-induced genotoxicity in marine diatom (*Chaetoceros tenuissimus*). Environmental Science and Pollution Research 23 (3), 2770–2777.
Shurin, J.B., Gruner, D.S., Hillebrand, H., 2006. All wet or dried up? Real differences between aquatic and terrestrial food webs. Proceedings of the Royal Society B: Biological Sciences 273 (1582), 1–9.
Singh, G., Patidar, S.K., 2018. Microalgae harvesting techniques: A review. Journal of environmental management 217, 499–508.
Spilling, K., 2020. Basic Methods for Isolating and Culturing Microalgae. Methods in Molecular Biology 1980, 35–39.
Suman, T.Y., Rajasree, S.R., Kirubagaran, R., 2015. Evaluation of zinc oxide nanoparticles toxicity on marine algae *Chlorella vulgaris* through flow cytometric, cytotoxicity and oxidative stress analysis. Ecotoxicology and environmental safety 113, 23–30.
Tang, Y., Xin, H., Yang, S., Guo, M., Malkoske, T., Yin, D., Xia, S., 2018. Environmental risks of ZnO nanoparticle exposure on *Microcystis aeruginosa*: toxic effects and environmental feedback. Aquatic toxicology 204, 19–26.
Tato, T., Beiras, R., 2019. The use of the marine microalga *Tisochrysis lutea* (T-iso) in standard toxicity tests; comparative sensitivity with other test species. Frontiers in Marine. Science 488.

Tomaru, Y., Shirai, Y., Toyoda, K., Nagasaki, K., 2011. Isolation and characterization of a single-stranded DNA virus infecting the marine planktonic diatom *Chaetoceros tenuissimus*. Aquatic Microbial Ecology 64, 175–184.

Turan, N.B., Erkan, H.S., Engin, G.O., Bilgili, M.S., 2019. Nanoparticles in the aquatic environment: Usage, properties, transformation and toxicity—A review. Process safety and environmental protection 130, 238–249.

Wang, X., Li, Y., Wei, S., Pan, L., Miao, J., Lin, Y., Wu, J., 2021. Acute toxic effect of typical chemicals and ecological risk assessment based on two marine microalgae, *Phaeodactylum tricornutum* and *Platymonas subcordiformis*. Environmental Toxicology and Pharmacology 85, 103649.

Wang, Y., Zhu, X., Lao, Y., Lv, X., Tao, Y., Huang, B., Wang, J., Zhou, J., Cai, Z., 2016. TiO_2 nanoparticles in the marine environment: Physical effects responsible for the toxicity on algae *Phaeodactylum tricornutum*. Science of the Total Environment 15 (565), 818–826.

Wu, D., Yang, S., Du, W., Yin, Y., Zhang, J., Guo, H., 2019. Effects of titanium dioxide nanoparticles on Microcystis aeruginosa and microcystins production and release. Journal of hazardous materials 377, 1–7.

Yamagishi, T., Yamaguchi, H., Suzuki, S., Horie, Y., Tatarazako, N., Baskin, T.I., 2017. Cell reproductive patterns in the green alga *Pseudokirchneriella subcapitata* (= *Selenastrum capricornutum*) and their variations under exposure to the typical toxicants potassium dichromate and 3, 5-DCP. PLoS One 12 (2), e0171259.

Yang, W., Gao, P., Ma, G., Huang, J., Wu, Y., Wan, L., Ding, H., Zhang, W., 2021. Transcriptome analysis of the toxic mechanism of nanoplastics on growth, photosynthesis and oxidative stress of microalga *Chlorella pyrenoidosa* during chronic exposure. Environmental Pollution 284, 117413.

Yu, C., Irudayaraj, J., 2005. Spectroscopic characterization of microorganisms by Fourier transform infrared microspectroscopy. Biopolymers 77 (6), 368–377.